Research Square

Preprints are preliminary reports that have not undergone peer review.
They should not be considered conclusive, used to inform clinical practice,
or referenced by the media as validated information.

SLC35G1 overexpression inhibits colorectal cancer cell proliferation and motility and reduces WDHD1 expression

ZHILIANG Chen
Shaoxing People's Hospital
LIFENG HU
Shaoxing People's Hospital
GUOJIANG TIAN
Shaoxing People's Hospital
QI WANG
Shaoxing People's Hospital
JIANG LIU
liujiang230822@163.com

Shaoxing People's Hospital

Research Article

Keywords: SLC35G1, Colon cancer, HT-29, SW-620, WDHD1

Posted Date: November 23rd, 2026

DOI: https://doi.org/10.21203/rs.3.rs-11436939/v1

License: This work is licensed under a Creative Commons Attribution 4.0 International License.
Read Full License

Additional Declarations: No competing interests reported.

SLC35G1 overexpression inhibits colorectal cancer cell proliferation and motility and reduces WDHD1 expression

ZHILIANG CHEN[1], LIFENG HU[1], GUOJIANG TIAN[1], QI WANG[1] and JIANG LIU[2]

[1]Department of Anorectal Surgery, Shaoxing People's Hospital, Shaoxing, China;
[2]Division of Colorectal Surgery, Shaoxing People's Hospital, Shaoxing, Zhejiang 312000, P.R. China

*Correspondence to:*DrJiang Liu, 568 Zhongxing North Road, Shaoxing, Zhejiang, 312000, P.R. China.
E-mail: liujiang230822@163.com

Abstract

Aim: To explore the role of solute carrier family 35 member G1 (*SLC35G1)* in colon cancer occurrence and development.

Materials and methods: Bioinformatic analysis was conducted using the GSE39582 dataset fromthe Gene Expression Omnibus database. SLC35G1was selected asthe research gene for Gene Ontology and Kyoto Encyclopedia of Genes and Genomes enrichment analyses, using R for bioinformatics. SLC35G1 or si-WD repeat and HMG-box DNA-binding protein 1 (WDHD1) were transfected into HT-29 and SW-620 cells, and their biological activities were observed. Cell proliferation, apoptosis, invasion, and migration were measured using MTT, flow cytometry, and Transwell assays, respectively, and relative gene and protein expression was evaluated using reverse transcription-quantitative PCR(RT-qPCR) and western blotting.

Results: SLC35G1 expression was closely associated with WDHD1 expression. Following the transfection of SLC35G1 into cells, cell proliferation, invasion, and migration abilities were significantly reduced, whereas cell apoptosis was significantly

increased (P<0.001). RT-qPCR and western blotting showed that when SLC35G1 expression increased, WDHD1expressionsignificantly decreased (P<0.001). However, when si-WDHD1 and SLC35G1were simultaneously transfected into the cells, the effect was consistent with the inhibitory effect of SLC35G1 alone on colon cancer. Conclusion: SLC35G1 inhibits biological activities of colon cancer cells by suppressing WDHD1.

Key words: SLC35G1, Colon cancer, HT-29, SW-620, WDHD1

Running Title: SLC35G1 and colon cancer

Introduction

Colorectal cancer (CRC) plays the most prevalent malignant tumor of the digestive system, with the rectum and sigmoid colon as the primary sites of occurrence. In Western countries, it constitutes a major cause of cancer incidence and mortality, and is the fifth leading cause of cancer-related mortality in China (Yu et al., 2024). Approximately 60% of patients with CRC experience metastasis, resulting in a significantly higher mortality rate (Shi et al., 2015).Enhancing the effectiveness of treatment strategies can significantly improve the survival rate of patients with CRC. Therefore, it is important to investigate the mechanisms underlying of CRC to identify potential therapeutic targets. CRC is one of the most common causes of cancer-related mortality and has a long latency period(Stoffel and Murphy, 2020). Surgical resection is a common curative treatment for CRC, but many patients remain undiagnosed because of the hidden nature of the disease, which results in the loss of early surgical opportunities (Ahmed et al., 2022). Early screening for CRC can reverse this phenomenon, as early detection of CRC significantly improves survival rates. When cancer is detected at a localized stage and treated surgically, the 5-year survival rate can reach 90% (Gupta, 2022). However, screening for CRC primarily targets individuals

aged >50 years, while the incidence of CRC in individuals aged <50 years is increasing annually (Krzeczewski et al., 2021). Despite the existence of tumor markers, there are still limitations and reliability issues in diagnosis, indicating the urgent need for the development of new indicators to predict the CRC. A study conducted antibody differential analysis of plasma samples from patients with CRCand healthy individuals, identifying 78 potential early detection markers for CRC, 32 of which were confirmed in control, colorectal adenoma,and cancer diagnosis samples (Rho et al., 2018). However, the clinical valuesof these biomarkers remain unclear.

Bioinformatic analysis is an invaluable approach for comprehensively analyzing large-scale databases, including intricate genetic information. In the present study, advanced bioinformatics techniques were used to identify potential CRC biomarkers. The Gene Expression Omnibus (GEO) database is an open repository that allows researchers to access and select appropriate mRNA expression profiles. Online analysis tools are available to detect discrepancies between tumor and normal tissues. In the present study, the GSE39582 dataset(colon cancer data)was selected for bioinformatics analysis, specifically targeting the highly divergent solute carrier family 35 member G1 (*SLC35G1*) gene and delineating its potential involvement in signaling pathways associated with CRC. Subsequently, clinical sample validation was conducted. To corroborate the findings of the bioinformatics analysis, HT-29 and SW-620 CRC cell lines were used. Following SLC35G1 overexpression, alterations in cellular biology were observed, and reverse transcription quantitative polymerase chain reaction(RT-qPCR) and western blotting(WB) were used to evaluate the relevant geneand proteinlevels. This study aimedto provide a theoretical basis for future investigations into clinically targeted drug development for CRC.

Materials and methods

Gene information. The GEO database is an international repository of genetic information that includes microarray and next-generation sequencing data(Barrett et al., 2023).The GSE39582 dataset consisting of 586CRC samples was used in this study.

Data preprocessing. The GSE39582 dataset was downloaded from the GEO database and expression levels of the probe control genes were obtained using gene platform annotations. The data were processed by removing missing values, background correction, and log2 transformation in preparation for further analyses.

Relationship between SLC35G1 gene expression and survival prognosis. Based on the median expression level of SLC35G1, the dataset was divided into two groups:high and low expression levels. The survival time and status of the patients in the two groups were recorded, and Kaplan-Meier (KM) survival analysis was performed to compare the overall survival differences between the groups. Univariate and multivariate Cox regression analyses were performed to determine the effects of SLC35G1 expression on patient survival.

Heat map of SLC35G1-associated genes. Using the Limma package, differentially expressed genes (|fold change|>1.4-fold; P<0.05) were identified between the high and low SLC35G1 expression groups, and a heat map of these differentially expressed genes was generated.

Enrichment analysis of SLC35G1-associated genes. The ClusterProfiler package in Bioconductor was used to perform Gene Ontology (GO) and Kyoto Encyclopedia of Genes and Genomes (KEGG) pathway enrichment analyses for differentially expressed genes. An enrichment bubble plot was created to visualize the results.

Protein-protein interaction (PPI) network construction and core protein selection. Differentially expressed genes were entered into the Search Tool for the Retrieval of Interacting Genes (STRING) database to construct the PPI network. The resulting network was visualized using Cystoscopes 3.9.1 software. A confidence score of>0.9 was defined as a valid interaction.

Clinical sample collection. Twenty patients with CRCadmitted to our hospital between

June and December 2021 were enrolled in this study. Cancerous and adjacent normal tissues were collected, fixed in 4% paraformaldehyde, embedded in paraffin, and sectioned (4 μm). This study was approved by the Ethics Committee of the Shaoxing People's Hospital (No.20201023-6). TNM staging in our cohort was as follows: stage I–II, 9 patients; and stage III–IV, 11 patients.

Immunohistochemical detection of SLC35G1 protein expression. Immunohistochemical staining for SLC35G1 was performed using an SP Immunohistochemistry (IHC) Kit (Beijing Baiao Laibo Technology Co. Ltd., Beijing, China) ready-to-use IIHCSP reagent), according to the manufacturer's instructions. Following staining, observations were made under a microscope (CX-23, Olympus, Japan; magnification, ×100) and ImageJ v1.8 software (National Institutes of Health) was used to analyze the integrated optical density values.

Experimental cell lines. HT-29 and SW-620 cellswere obtained from Shanghai Xinyu Biotechnology Co. Ltd.

Main reagents and instruments. SLC35G1, si-negative control (si-NC), si-WD repeat, and HMG-box DNA-binding protein 1 (WDHD1) were synthesized by Invitrogen (Thermo Fisher Scientific, Inc). SLC35G1 (cat. no. orb1559181, Wuhan Booute Biotechnology Co. Ltd., Wuhan, China, 1:1,000), WDHD1 (cat. no. ab224221, Abcam, USA, 1: 1,000), GAPDH (cat. no. ab8245, Abcam, 1: 1,000), a secondary antibody (cat. no. ab288151, Abcam) were used. MTT and dimethyl sulfoxide (DMSO) were purchased from Shanghai Huiying Biotechnology Co. Ltd. An inverted fluorescence microscope (MLB) was purchased from Nikon (Tokyo, Japan).

Cell culture. Frozen SW-620 and HT-29 cells were rapidly dissolved in a 37 °C water bath, centrifuged, and the supernatant discarded. RPMI culture medium was added and the cells were cultured in an incubator at 37 °C with 5% CO_2 and saturated humidity for adherent growth. The medium was replaced on the following day and once the cells

reached 90% confluence, perform cell passaging. The cells were passaged at 37 °C and stored for future use.

Cell grouping. HT-29 and SW-620 cells were transfected with NC, SLC35G1 (transfected with SLC35G1), si-NC (transfected with si-NC), pcDNA3.1 (transfected with pcDNA3.1 empty vector control), and SLC35G1+si-WDHD1 (transfected with SLC35G1 and si-WDHD1) groups. Following cell fusion, pcDNA3.1 groups were transfected with pcDNA3.1 empty vector control; SLC35G1 and SLC35G1+si-WDHD1 groups were transfected with SLC35G1 by pcDNA3.1. Next, Depending on instructions of Lipofectamine 3000 (Invitrogen, USA), 200 μl transfection solution and 4 μl liposomes were added according to the si-NC and si-WDHD1, and cells were cultured for 36 h. The culture medium was replaced the next day and using RT-qPCR assay to detect successful transfections rates.

MTT assay. After 48 h of treatment, the cells in each group were treated with 10 ml MTT solution and cultured for 4 h. Following the addition of 15 μl of DMSO and shaking, the absorbance was measured at a wavelength of 570 nm using an enzyme label reader to calculate the cell proliferation rate.

5-Ethynyl-2'-deoxyuridine (EdU) cell proliferation detection. Cells were seeded in a 96-well plate at a density of 5,000 cells/well and cultured for 24 h. Following EdU labeling, cell fixation, and Apollo staining, fluorescence microscopy was used to observe and photograph the cells. The cell nuclei appeared blue and proliferating cells appeared red under a fluorescence microscope.

Transwell chamber assay for CRC cell invasion. A Matrigel (KeyGEN BioTECH, Nanjing, China) diluted to 200 μg/mL (0.25 mg/mL) was added to the upper transwell chamber and allowed to solidify at 37 °C. The cell density was 1×10^5/ml. The cell suspension was added to the upper chamber, a small amount of fetal bovine serum culture medium was added to the lower chamber, and cells were cultured at 37 °C for

48 h. The culture medium and remaining cells were removed, and 0.1% crystal violet staining was performed. Images were captured and HT-29 and SW-620 invasive cells were counted under an inverted microscope in four random fields.

Transwell chamber assay for CRC cell migration ability. After 24 h of transfection, cells from each group were resuspended in cell suspension at a concentration of 1×10^5 cells/ml. Transwell chambers were prepared by serum-free medium in the upper chamber and 100 μl of culture medium containing 10% fetal bovine serum to the lower chamber. The chambers were incubated at at 37 ℃ with 5% CO_2 for 24 h. After fixation with 4% paraformaldehyde and crystal violet staining, the chambers were observed under an optical microscope (CX-23, Olympus, Japan). Five random fields were selected for cell counting and cell numbers represented cell migration ability.

Annexin V-FITC/PI flow cytometry assay. The cells were digested with 0.25% trypsin without EDTA and 1×10^6 cells were counted. The cells were washed twice with cold PBS at 1,000 × g and 4 °C for 10 min each. The cells were then resuspended in 100 μlof binding buffer and incubated in the dark at room temperature for 15 min with 5 μL PI (Propidium Iodide) and Annexin V-FITC. The detection was completed within 1 h.

RT-qPCR for SLC35G1 and WDHD1 gene expression detection. After 48 h of treatment, the cells were digested with trypsin, washed with PBS. The cell suspension was placed in an EP tube containing 1×10^6 of cells and total cell mRNA was extracted using the TRIzolreagent.Reverse transcription of cDNA was performed using β-Actin as the internal reference gene. Amplification was performed under the following conditions: 95 °C for 15 s, 60 °C for 28 s (annealing), 72 °C for 30 s, a total of 40 cycles. The primer sequences are listed in Table 1.

Table 1. Primer sequence

Gene Name	F:(5'-3')	R:(5'-3')
SLC35G1	TGGCTCTGCCTTTCCTCG	GAACACACATCGAAACGCAC
WDHD1	AGGTCGTCCTAGACAGCG	GCATGGGTCCATCATAAA

β-Actin	CATTAAGGAGAAGCTGTGCT	GTTGAAGGTAGTTTCGTGGA

Immunoblot detection of SLC35G1 and WDHD1 protein levels (WB assay). After 48 h of treatment, the cells were lysed on ice for 60 min and centrifuged at 13,000× g for 10 min. Protein concentration was measured using a BCA kit (KGA902, Jiangsu Kaiji Biotechnology Co. Ltd, Nanjing, China).Next, 40 μg proteins were separated on a 10% SDS-PAGE gel. The PVDF membranes were soaked in methanol for 10 min and washed with PBS for 5 min each. Add a blocking solution containing 5% skim milk powder, shake the shaker for 1.5-2 hours; after the blocking is complete, wash the membrane with TBST for 10 minutes x 3 times. Primary antibody SLC35G1 (cat. no. ANT-196-25UL, Thermo Fisher Scientific, 1:1,000), WDHD1 (cat. no. ab224221, Abcam, 1:1,000), and GAPDH (cat. no. ab181602, Abcam, 1:1,000)were added, followed by incubation with goat anti-rabbit (dilution, 1:1,000) and peroxidase-conjugated (dilution, 1: 1,000) secondary antibodies. The membrane was then immersed in an enhanced chemiluminescence working solution and images were obtained. The grayscale value ratio of target proteins to the internal reference was quantified using ImageJ software (version 1.54).

Statistical analysis. R 4.2.3 language was used for GO and KEGG analyses. PSS software (version 23.0) was used for statistical analysis. One-way ANOVA with Tukey's post-hoc test was used to analyze the statistical significance between the groups. $P<0.05$was considered statistically significant. Data are expressed as mean ± standard deviation (SD).

Results

Differential gene analysis. After analyzing the tissues of 586 patients with CRC, the results showed that SLC35G1, discoidal, CUB, LCCL domain containing 2, inhibin subunit beta B, LY6/PLAUR domain containing 6,and XK-related X-linked all had statistical significance in CRC compared with those in adjacent normal tissues, with

SLC35G1 exhibiting the most statistically significant difference. Therefore, SLC35G1 was selected for subsequent experiments. The detailed data are presented in Table 2.

Table 2. Differential gene analysis

ID	Gender	Age	T	N	SigNum
SLC35G1	0.882689	0.2317222	0.0361548	0.002186	2
DCBLD2	0.6798967	0.4729928	0.0427672	0.06781	1
INHBB	0.653075	0.4576624	0.0990442	0.0288241	1
LYPD6	0.7370956	0.152373	0.1484912	0.0007531	1
XKRX	0.0765103	0.5903799	0.0175571	0.2002434	1

Relationship between SLC35G1 and prognosis of patients with CRC. In this study, gene expression in the tissues of 586patients with CRC was analyzed to investigate the association between SLC35G1 expression and patient prognosis. Based on the median value of SLC35G1 expression, samples were divided into high (n=293) and low (n=293) expression groups. KM analysis revealed that SLC35G1expression was positively correlated with patient survival in the dataset, indicating that patients with high SLC35G1 expression had significantly higher survival rates ($P<0.05$; Fig. 1).

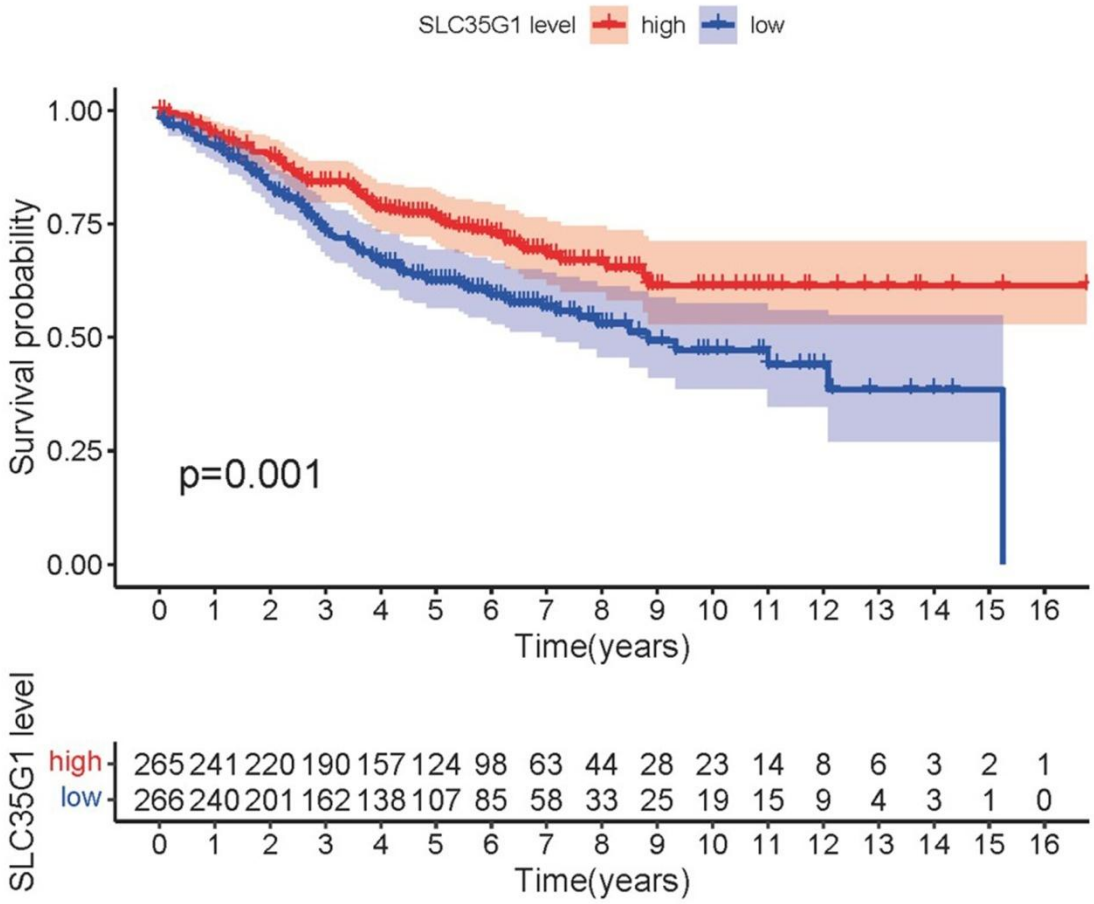


Figure 1. Relationship between SLC35G1 and Prognosis of Patients with Colorectal Cancer

Cox regression analysis was performed to further examine the factors affecting overall survival. Univariate Cox regression analysis (Fig. 2A) revealed that age, T stage, N stage, and SLC35G1 expression were significantly associated with patient overall survival. Multivariate Cox regression analysis (Fig. 2B) showed that SLC35G1 expression level was an independent risk factor for prognosis(hazard ratio = 0.109, 95% confidence interval 0.025–0.476; P=0.003) and could serve as a predictive biomarker for overall survival in patients with CRC(Fig. 2).

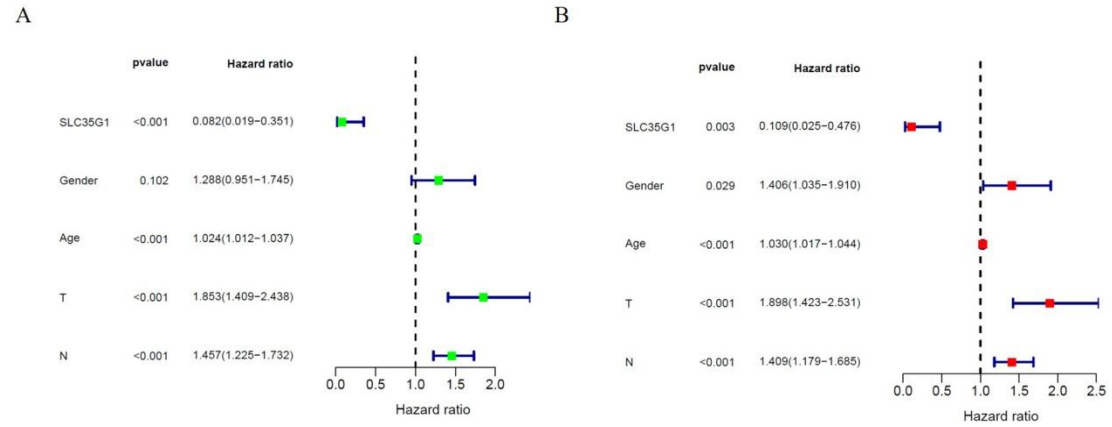
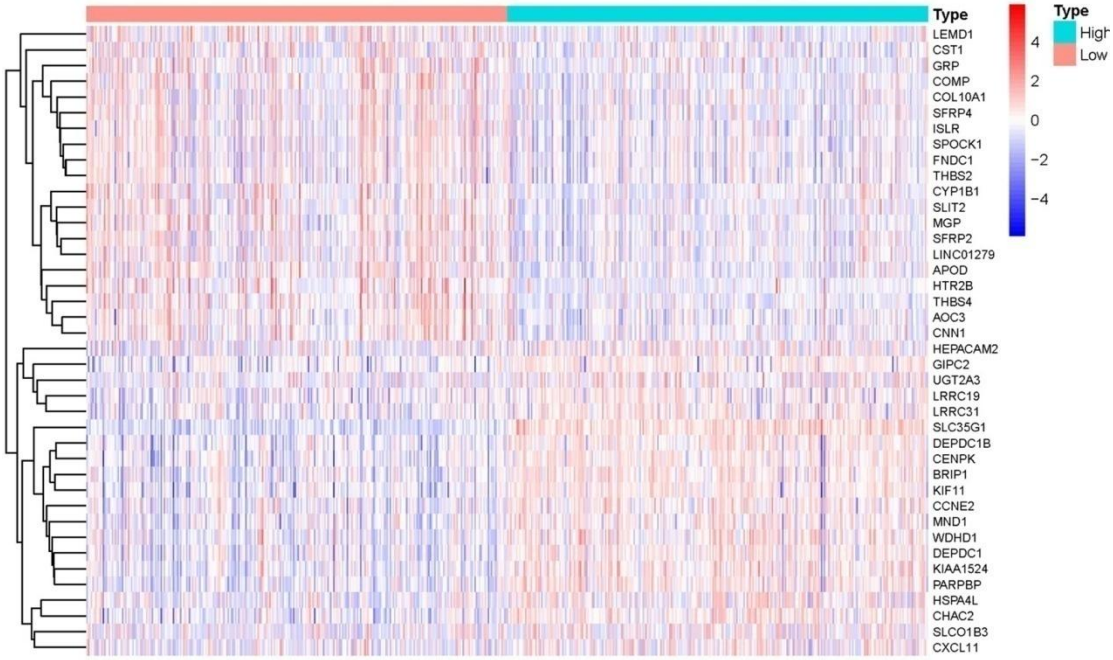


Figure 2. Colon Cancer Risk Factor Analysis

A. Cox univariate analysis

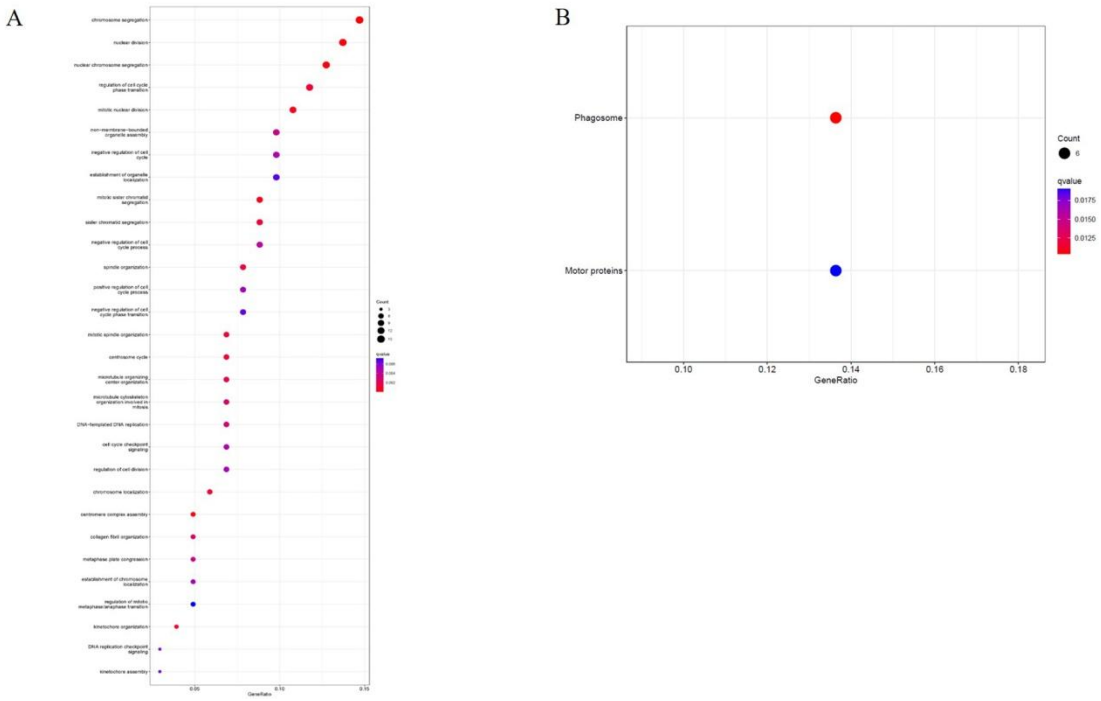
B. Cox multivariate analysis

Identification of differentially expressed genes associated with SLC35G1. Statistical analysis of the gene chip results from 586 samples identified 185 differentially expressed genes. Heatmaps were created to visualize the top 20 differentially expressed genes in the high and low SLC35G1 expression groups (Fig. 3). These genes may be associated with SLC35G1 function.

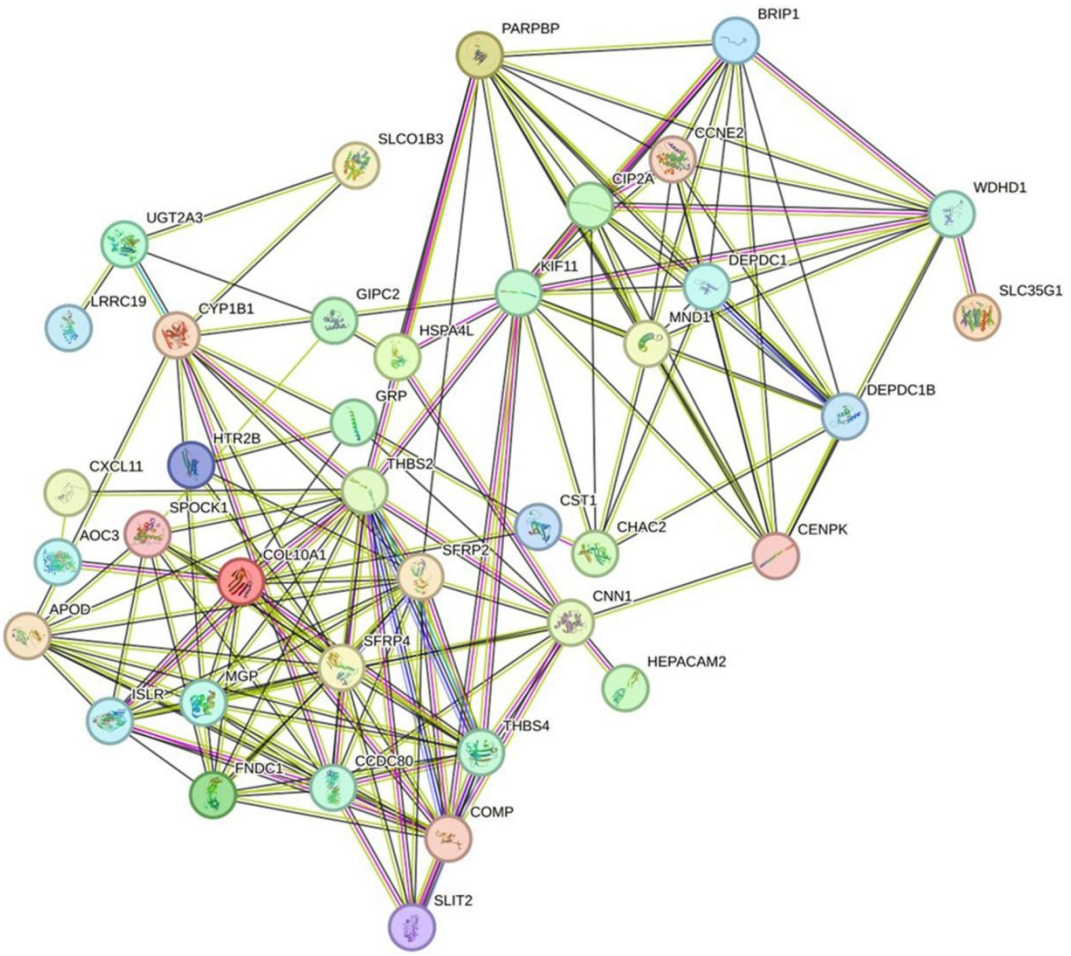


GO and KEGG pathway signal analysis. To further explore the potential mechanisms

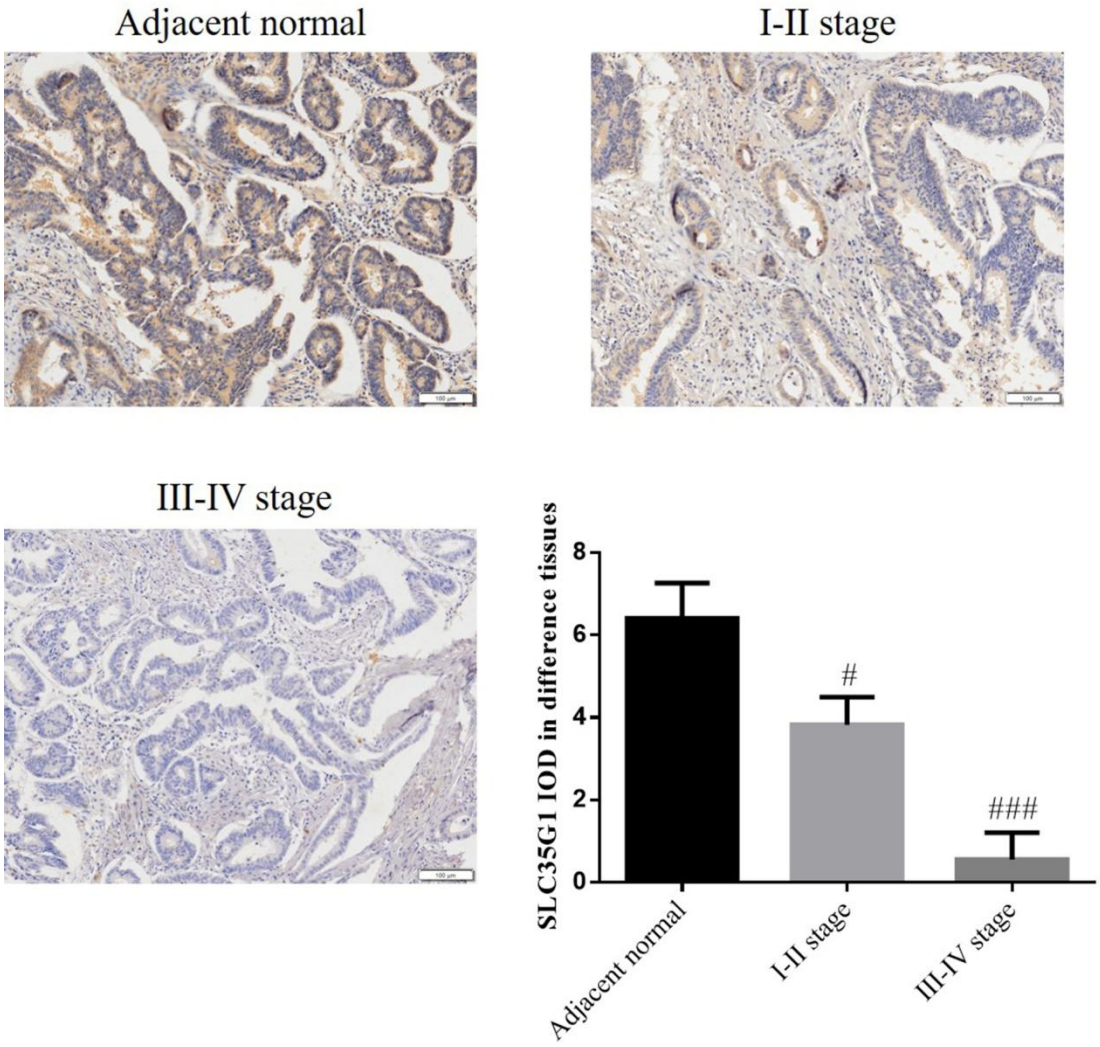
by which SLC35G1-related genes regulate the occurrence and development of CRC, functional enrichment analysis was conducted using GO and KEGG methods. GO analysis revealed that SLC35G1 was closely associated with molecular mechanisms, such as chromosome segregation, nuclear division, nuclear chromosome segregation, regulation of cell cycle phase transition, and mitotic nuclear division (Fig. 4A). KEGG analysis revealed that, among the 118 genes associated with SLC35G1, the main pathways involved were phagosomes and motor proteins (Fig. 4B).



Construction of a PPI network and identification of hub genes. To further explore the mechanisms involved in the function of SLC35G1, a PPI network was constructed using the STRING database. PPI analysis results (Fig. 5) showed a close correlation between SLC35G1 and WDHD1.

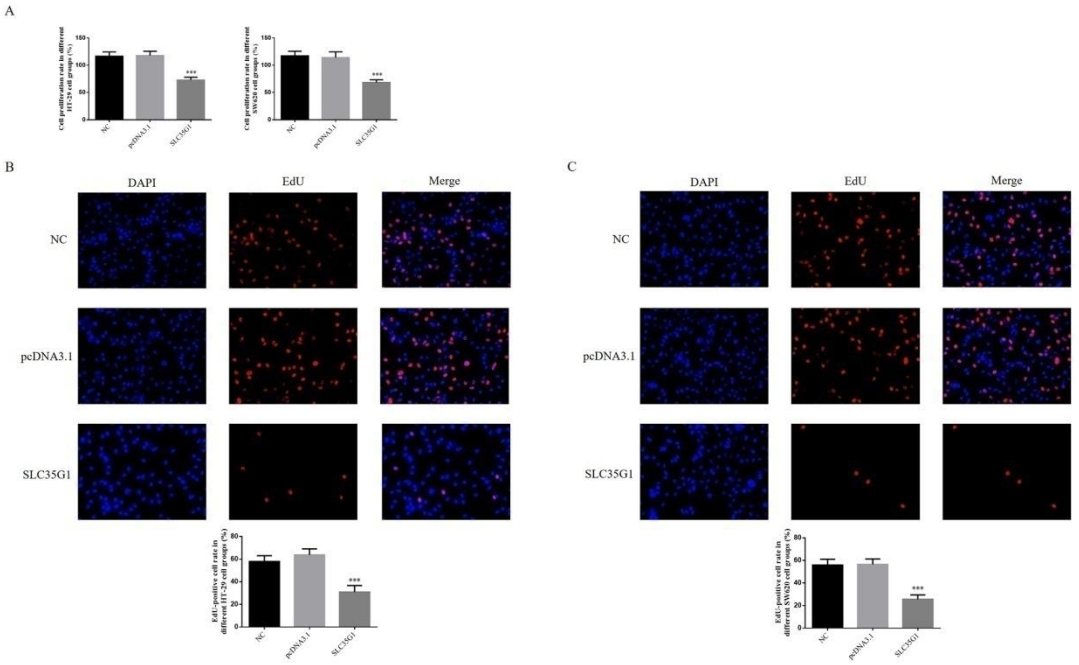


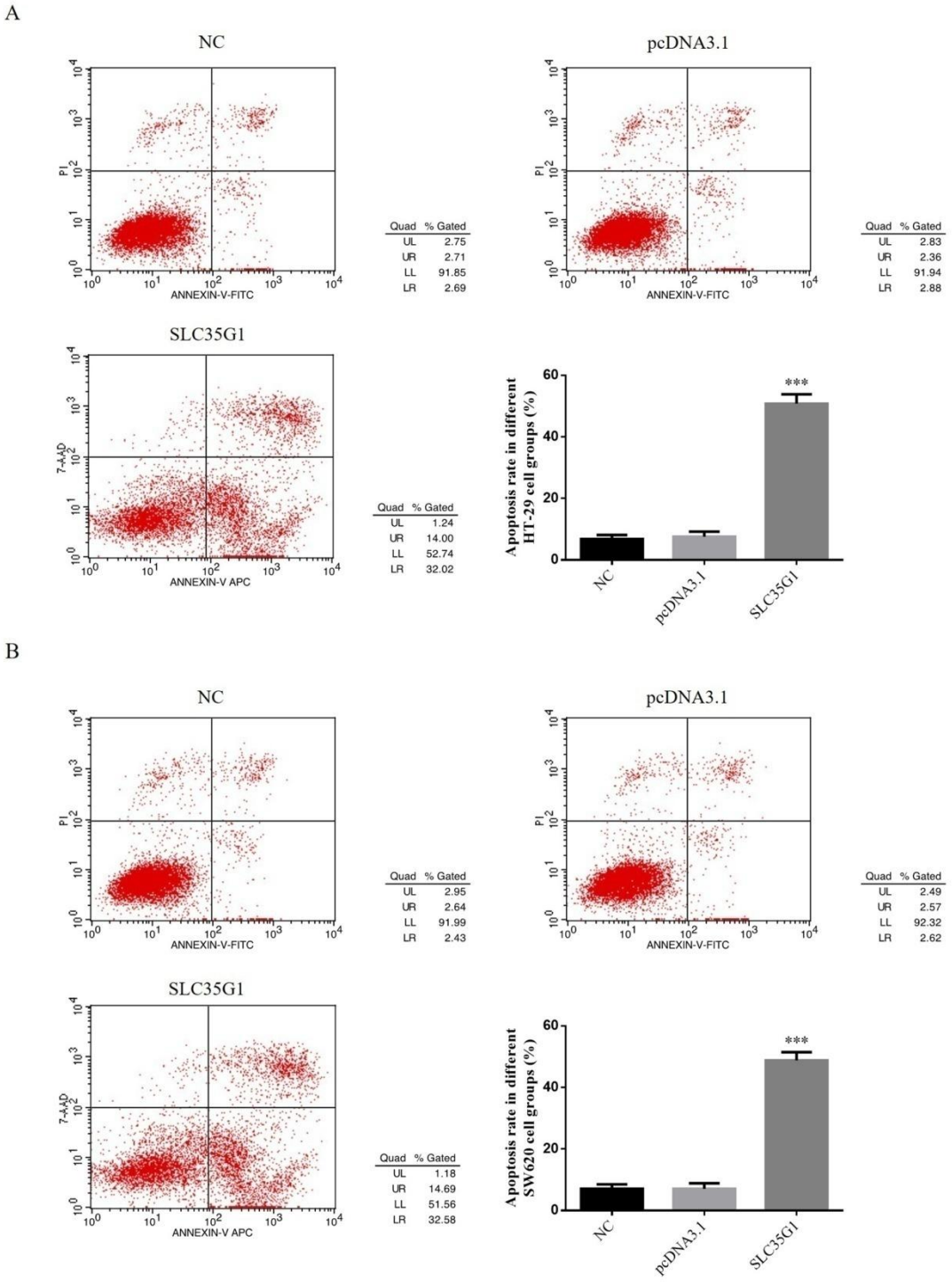
Clinical validation of SLC35G1 protein. The IHC results (Fig. 6) showed thatSLC35G1 wasexpressed in the cell nucleus and cytoplasm,and the protein expression of SLC35G1 was significantly decreased in stage I–II and III–IV CRC tissues ($P<0.05$, $P<0.001$; Fig. 6). These results confirmedthat SLC35G1was downregulatedin CRC tissues.



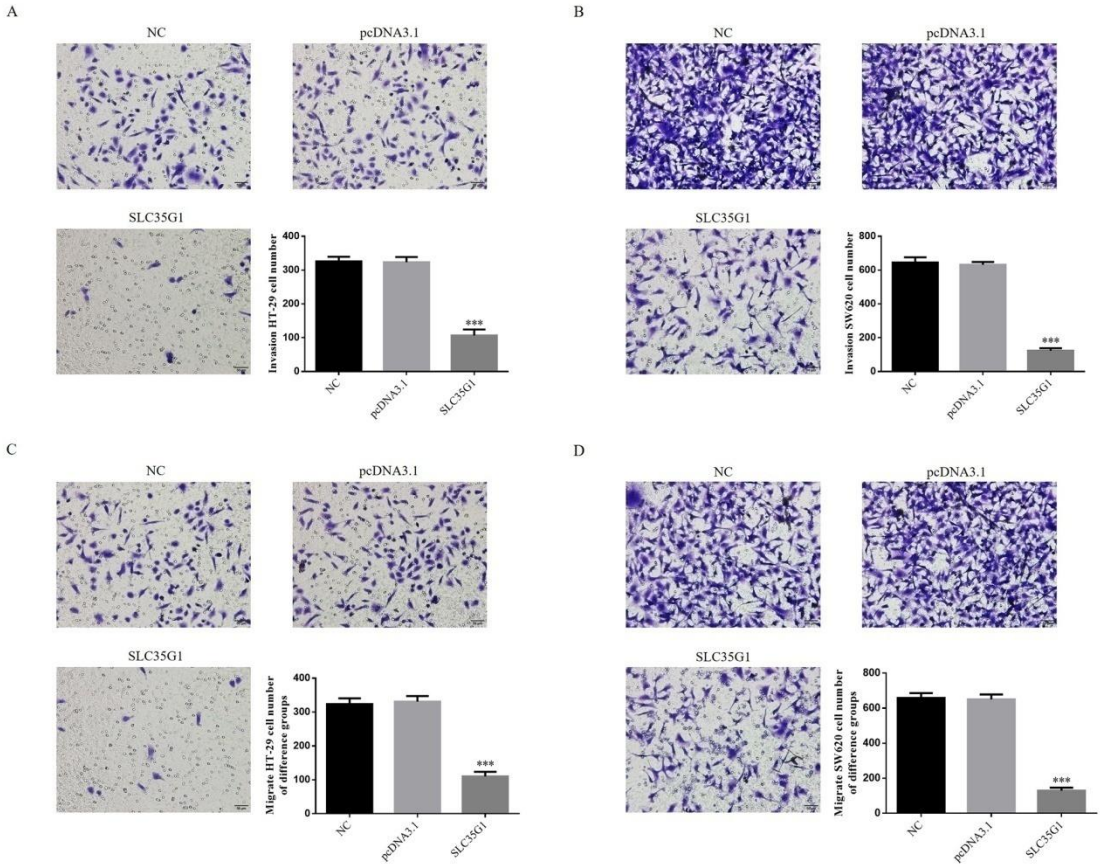
Effects of SLC35G1 overexpression on CRC cell proliferation. The MTT assay results demonstrated that the proliferation rates of HT-29 and SW-620 cells were significantly reduced in the SLC35G1 group ($P<0.001$, Fig. 7A). EdU staining revealed a significant decrease in the number of positive cells in the SLC35G1 group of HT-29 and SW-620 cells ($P<0.001$; Fig. 7B and C).

Effects of SLC35G1 overexpression on CRC cell apoptosis. Flow cytometry showed that the apoptotic rates of HT-29 and SW-620 cells significantly increased in the SLC35G1 group ($P<0.001$; Fig. 8A and B).

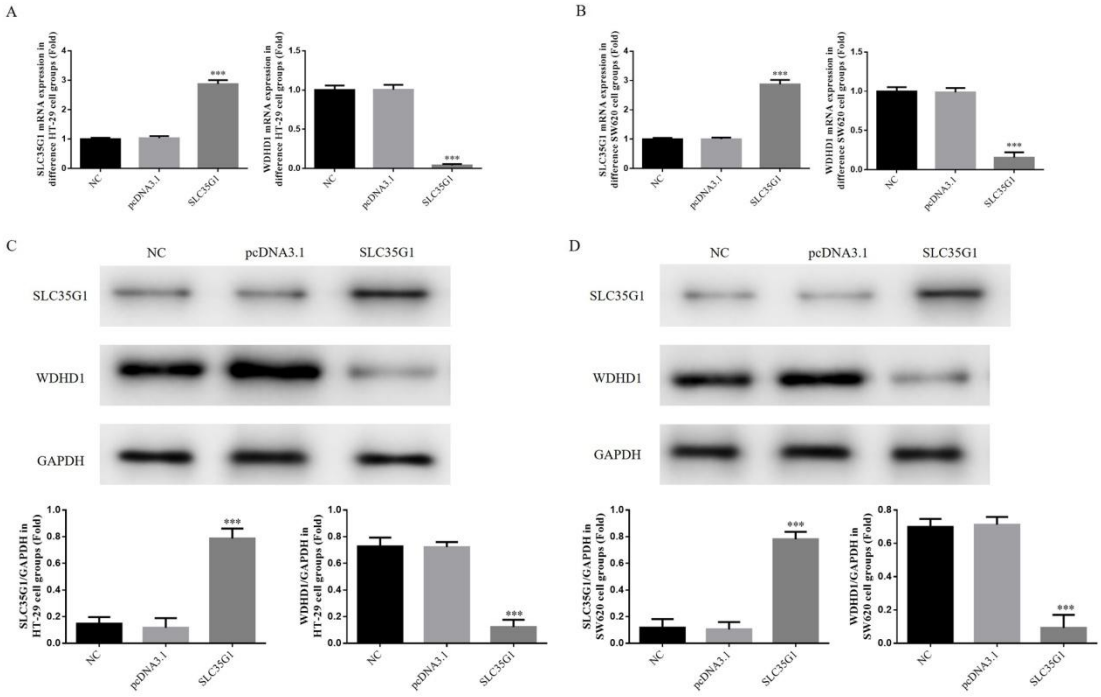

A
B
C
DAPI
EdU
Merge
NC
pcDNA3.1
SLC35G1
***



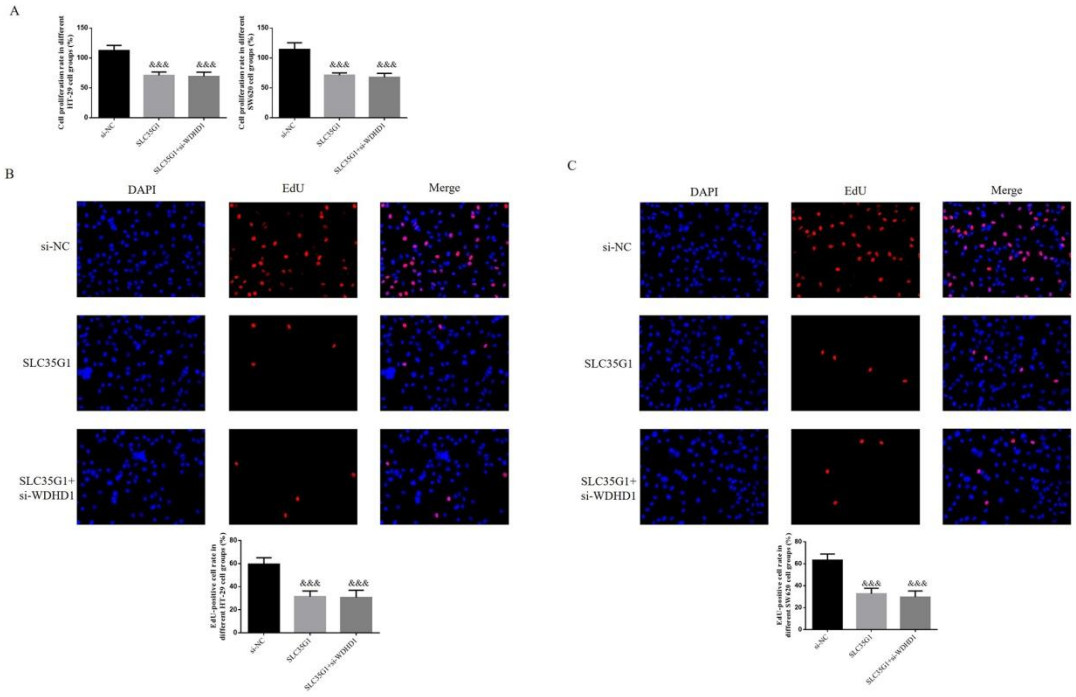
Effects of SLC35G1 overexpression on CRC cell invasion and migration. Transwell assay results demonstrated that the number of invasive cells was significantly reduced in the SLC35G1 group of HT-29 and SW-620 cells (P<0.001; Fig. 9A and B). Similarly, the number of migratory cells was significantly reduced in the SLC35G1 group of HT-29 and SW-620 cells (P<0.001; Fig. 9C and D).



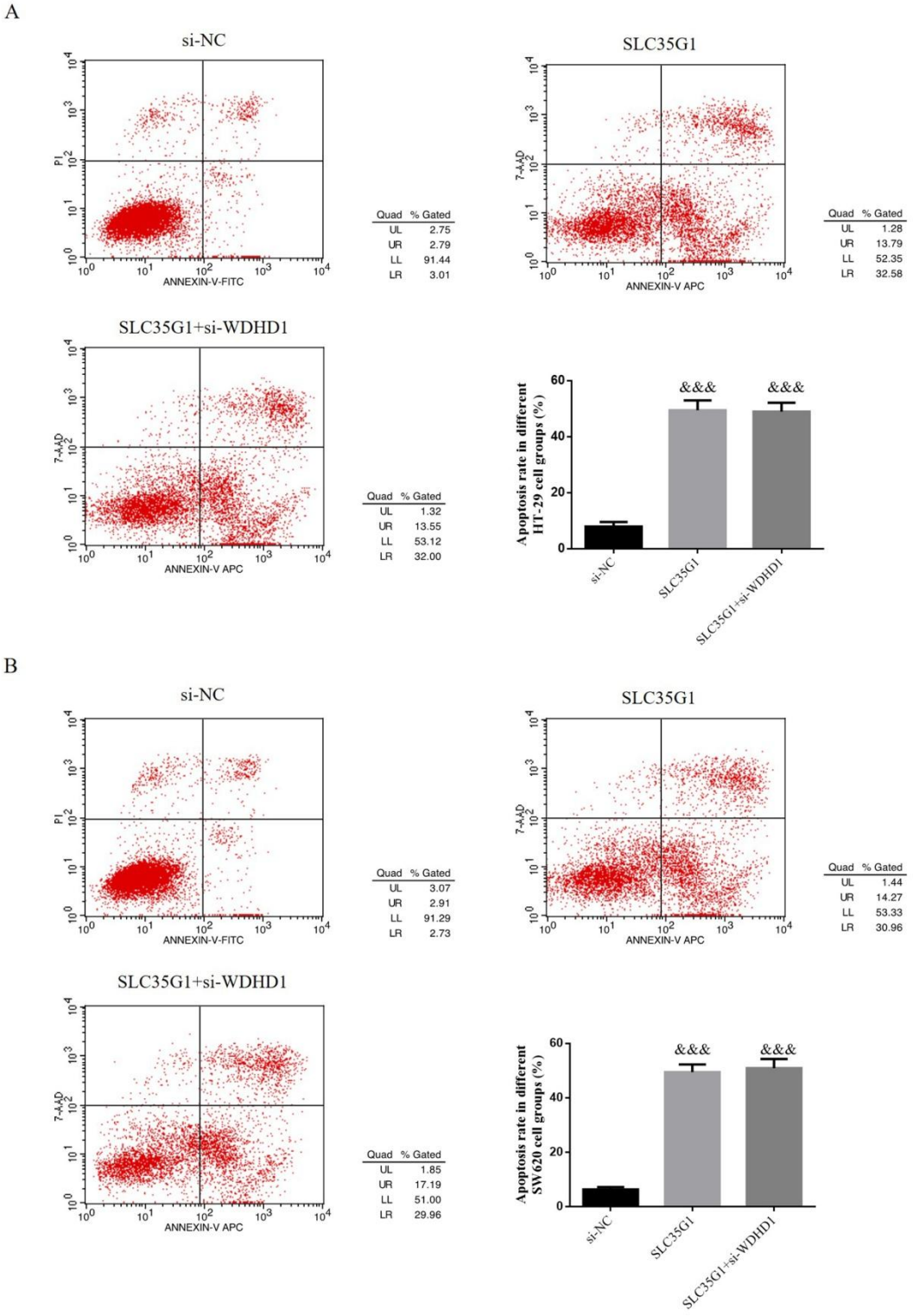
Effects of SLC35G1 overexpression on related genes and proteins. RT-qPCR results showed that the SLC35G1 gene level was significantly increased, whereas the expression of the *WDHD1* gene was significantly decreased inHT-29 and SW-620 cells in the SLC35G1 group (P<0.001;Fig. 10A and B). WB results demonstrated that the SLC35G1 protein levelwas significantly increased, whereasthe WDHD1 protein levelwas significantly decreased inHT-29 and SW-620 cells in the SLC35G1 group (P<0.001;Fig. 10C and D).



Role of si-WDHD1 in inhibiting CRC proliferation by SLC35G1 overexpression. The proliferation rates of HT-29 and SW-620 cells in the SLC35G1 and SLC35G1+si-WDHD1 groups were reduced ($P<0.001$; Fig. 11A). EdU staining showed that the number of HT-29 and SW-620 cells positive for SLC35G1 and SLC35G1+si-WDHD1 was significantly reduced ($P<0.001$; Fig. 11B and C). There were no significant differences in cell proliferation rates and EdU-positive HT-29 and SW-620 cell numbers between the SLC35G1 and SLC35G1+si-WDHD1 groups, suggesting that SLC35G1 inhibits CRC cell proliferation by downregulating WDHD1 expression.

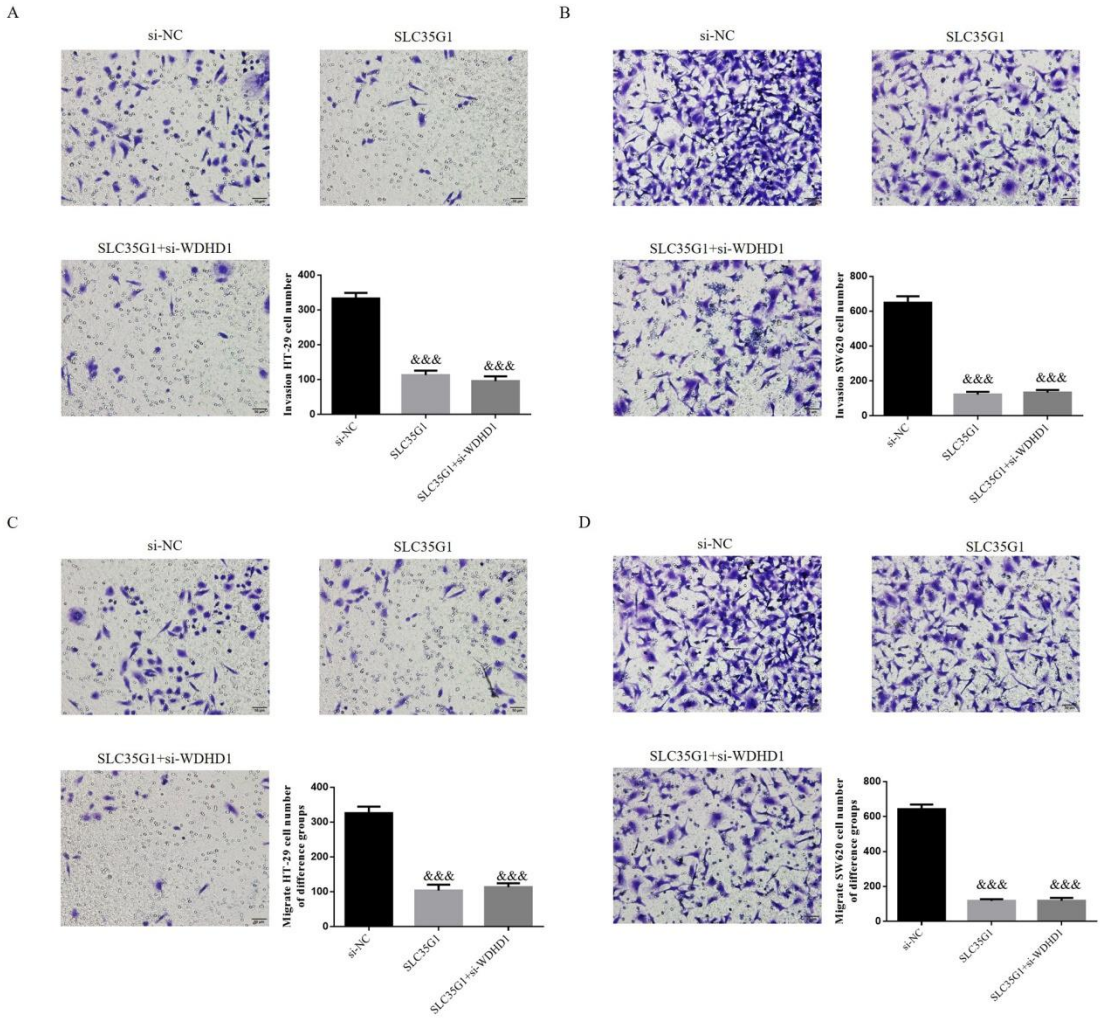


Effects of si-WDHD1 in promoting CRC cell apoptosis by SLC35G1 overexpression. Compared withthe si-NC group, the apoptotic rates of HT-29 and SW-620 cells in the SLC35G1 and SLC35G1+si-WDHD1 groups were significantly higher ($P<0.001$; Fig. 12A and B). There was no significant difference between the SLC35G1 and SLC35G1+si-WDHD1 groups, suggesting that SLC35G1 promoted CRC cell apoptosis by downregulating WDHD1 expression.



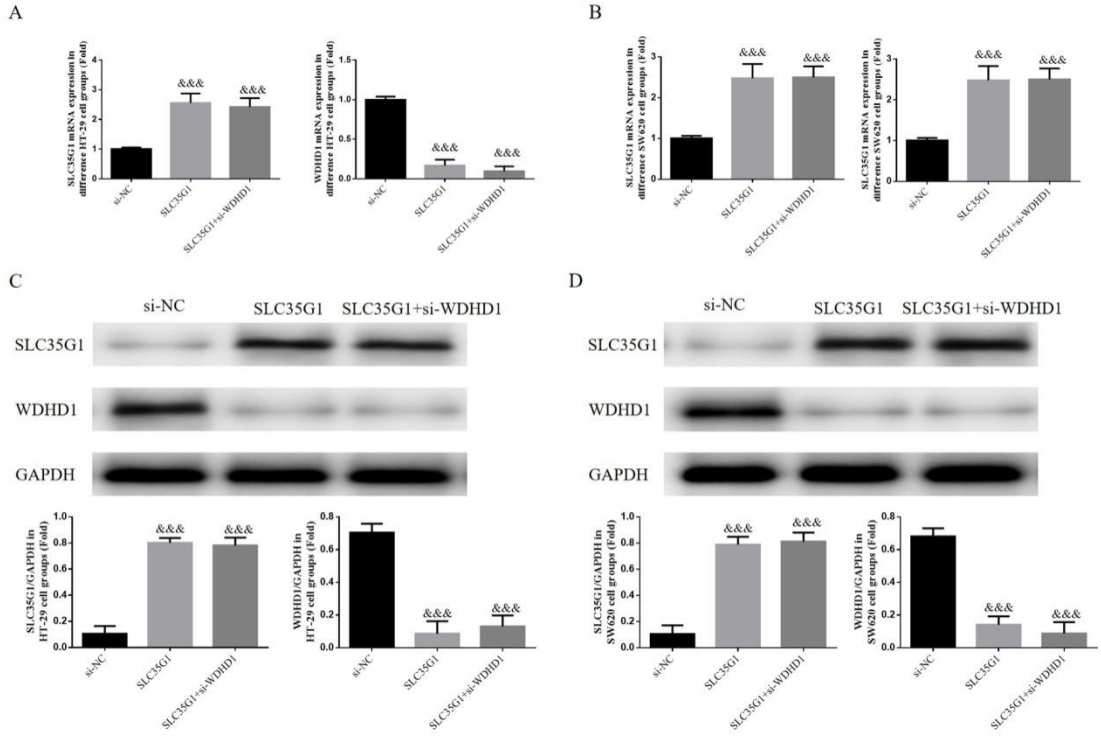
Effects of si-WDHD1 in inhibiting CRC cell invasion and migration by SLC35G1 overexpression. The number of invasive cells in the SLC35G1 and SLC35G1+si-WDHD1 groups of HT-29 and SW-620 cells were significantly inhibited (P<0.001; Fig.

13A and B). Simultaneously, the numbers of migrating HT-29 and SW-620 cells in the SLC35G1 and SLC35G1+si-WDHD1 groups were significantly reduced (P<0.001; Fig. 13C and D). There was no significant difference in the number of invasive and migrating cells between the SLC35G1 and SLC35G1+si-WDHD1 groups, suggesting that SLC35G1 inhibits CRC cell invasion and migration by downregulating WDHD1.



SLC35G1 and WDHD1 gene and protein levels. RT-qPCR results showed that*SLC35G1* gene expression was significantly increased, whereas*WDHD1* gene expression was significantly decreased in HT-29 and SW-620 cells in the SLC35G1 and SLC35G1+si-WDHD1 groups (P<0.001, respectively; Fig. 14A and B). WB results demonstrated that SLC35G1 protein levels were significantly increased, whereas WDHD1 protein expression was significantly decreased in HT-29 and SW-620 cells in the SLC35G1 and

SLC35G1+si-WDHD1 groups (P<0.001; Fig. 14C and D).



Discussion

In this study, SLC35G1 was found to be specific to patients with CRC. Previous studies have shown that SLC35G1 is a potential member of the drug/metabolite transport protein superfamily (Deng et al., 2020; Sherva et al., 2016) that can bind to the matrix and exchange calcium ions (Yuan et al., 2007). Analysis of the GSE39582 dataset from the Gene Expression Omnibus revealed associations between SLC35G1 expression, CRC prognosis, and clinicopathological characteristics. Clinical samples collected at our hospital were used for immunohistochemical evaluation of SLC35G1 protein expression, and the findings were consistent with the public dataset analysis. To further determine the effect of SLC35G1 on the biological activity of CRC cells, HT-29 and SW-620 cells were used. SLC35G1 overexpression inhibits cell proliferation by increasing apoptosis and effectively inhibits the invasion and migration of CRC cells. GO, KEGG, and PPI analyses revealed that SLC35G1 may regulate WDHD1 expression. RT-qPCR and WB revealed that SLC35G1 overexpression significantly

decreased WDHD1 expression.

WDHD1 is a ubiquitin ligase associated with tumor development and malignant phenotypes (Gong et al., 2020; Guo et al., 2023; Simon et al., 2020). WDHD1 is the human homolog of CTF4 in *Saccharomyces cerevisiae* (Sato et al., 2010). Its sequence was similar to that of CTF4, with 21% homology and 36% similarity in 722/1,129 aligned residues, respectively. Therefore, WDHD1 may share some or all the functions of its yeast counterpart to maintain genome stability and establish sister chromatid cohesion (Kilkenny et al., 2017). WDHD1 is mainly involved in regulating cellular DNA replication and the cell cycle (Jaramillo-Lambert et al., 2013; Liu et al., 2019). DNA replication in eukaryotic cells is mediated by a multi-protein complex called 'the replisome,' which consists of helicases, polymerases, and adaptor molecules. WDHD1 is a key adaptor molecule involved in DNA replication (Guan et al., 2017). WDHD1 is located near the origin of DNA replication and plays an important role in the initiation of DNA replication (Yoshizawa-Sugata and Masai, 2009; Zhu et al., 2007). Some researchers have suggested that WDHD1 may play a role in viral oncogene-induced replication and is associated with cell cycle checkpoint control, epithelial-mesenchymal transition, tumor growth, and metastasis (Zhou and Chen, 2021). In the present study, we found thatWDHD1 significantly decreasedSLC35G1 overexpression. However, when SLC35G1 overexpression and si-WDHD1 (WDHD1 knockout) were simultaneously transfected into CRC cells, there was no significant difference in cellular activity (proliferation, apoptosis, invasion, and migration) compared with the effect of SLC35G1 overexpression alone. However, this study has several limitations. It only discussed the SLC35G1 effects of mechanism in colon cancer; however, the effects of SLC35G1 on other cancer cell lines remain unclear. Future research should address these limitations in the future. The SLC35G1 mechanism in CRC also remains unclear, therefore, future research will also focus on therelationship between SLG35G1 and the mitochondrial pathway. Additionally, the downstream effects of WDHD1 are unclear; the present study only discuss the SLC35G1 effects in vitro, while in vivo effects are unclear. In future studies, we will address these limitations.

Conclusion

The present study showed that SLC35G1 suppressed the biological activity of CRC cells by inhibiting WDHD1, indicating its potential therapeutic significance in the treatment of CRC.

Statements and Declarations

Acknowledgements

Not applicable.

Funding

Not applicable

Authors' contributions

ZLC, LFH,and JL conceived and designed the study. GJT provided administrative support. GJT, QW, ZLC,and JL collected data. LFH, GJT, QW, and JL analyzed the data. ZLC, LFH, and GJT performed the experiments. QW revised the manuscript accordingly. QW and JL confirmed raw data authenticity. All the authors have read and approved the final manuscript.

Ethics approval and consent to participate

This study was conducted in accordance with the Declaration of Helsinki and was approved by the Ethics Committee of Shaoxing People's Hospital (approval no. 20201023-6). Informed consent was obtained from all participants.

Consent to publish

Not applicable.

Declaration of conflicting interest

The authors declared no potential conflicts of interest with respect to the research, authorship, and/or publication of this article

Data Availability Statement

The gene expression data analysed in this study are publicly available in the NCBI Gene Expression Omnibus under accession number GSE39582. Protein-protein interaction data were obtained from the STRING human protein association database (Homo sapiens; NCBI taxonomy identifier 9606), using an interaction confidence score >0.9. Functional annotations and pathway information were obtained from Gene Ontology (GO) and the Kyoto Encyclopedia of Genes and Genomes (KEGG), respectively, through the clusterProfiler package. Other data generated or analysed during this study are available from the corresponding author on reasonable request.

References

Ahmed A, Prothixene NVK, Charate Ret al.(2022) Inappropriate sinus tachycardia: etiology, pathophysiology, and management: JACC review topic of the week. Journal of the American College of Cardiology79(24):2450-2462.

Barrett T, Wilhite SE, Ledoux P, et al. (2013) NCBI GEO: archive for functional genomics data sets-update. Nucleic Acids Research41(Database issue): D991-D995.

Deng M, Chen Z, Tan J, et al. (2020) Down-regulation of SLC35C1 induces colon cancer through over-activating Wnt pathway. Journal of Cellular and Molecular Medicine24(5):3079-3090.

Gong L, Xiao M, He D, et al. (2020) WDHD1 leads to cisplatin resistance by promoting MAPRE2 ubiquitination in lung adenocarcinoma. Frontiers in Oncology10:461.

Guan C, Li J, Sun D, et al. (2017) The structure and polymerase-recognition mechanism of the crucial adaptor protein AND-1 in the human replisome. The Journal of Biological Chemistry292(23):9627-9636.

Guo X, Zhang H, Wang H, et al. (2023) Identification of key modules and hub genes involved in regulating the color of chicken breast meat using WGCNA. Animals (Basel). 13(14):2356.

Gupta S. (2022) Screening for colorectal cancer. Hematology/Oncology Clinics of North America36(3):393-414.

Jaramillo-Lambert A, Hao J, Xiao H, et al. (2013) Acidic nucleoplasmic DNA-binding protein (And-1) controls chromosome congression by regulating the assembly of centromere protein A (CENP-A) at centromeres. The Journal of Biological Chemistry288(3):1480-1488.

Kilkenny ML, Simon AC, Mainwaring et al. (2017) The human CTF4-orthologue AND-1 interacts with DNA polymerase α/primase via its unique C-terminal HMG box. Open Biology7(11):170217.

Krzeczewski B, Hassan C, Krzeczewska O, et al. (2021) Cost-effectiveness of colonoscopy in an organized screening program. Polish Archives of Internal Medicine131(2):128-135.

Liu B, Hu Y, Qin L, et al. (2019)MicroRNA-494-dependent WDHDI inhibition suppresses epithelial-mesenchymal transition, tumor growth and metastasis in cholangiocarcinoma. Digestive and Liver Disease51(3):397-411.

Rho JH, Ladd JJ, Li CI, et al. (2018) Protein and glycomic plasma markers for early detection of adenoma and colon cancer. Gut67(3):473-484.

Sato N, Koinuma J, Fujita M, et al. (2010) Activation of WD repeat and high-mobility group box DNA binding protein 1 in pulmonary and esophageal carcinogenesis. Clinical Cancer Research16(1):226-239.

Sherva R, Wang Q, Kranzler H, et al. (2016) Genome-wide association study of cannabis dependence severity, novel risk variants, and shared genetic risks. JAMA Psychiatry. 73(5):472-480.

Shi X, Chen G, Liu X, et al. (2015) Scutellarein inhibits cancer cell metastasis in vitro and attenuates the development of fibrosarcoma in vivo. International Journal of Molecular Medicine35(1):31-38.

Simon AK, Kummer S, Wild S, et al. (2020) The iron-sulfur helicase DDX11 promotes the generation of single-stranded DNA for CHK1 activation. Life Science Alliance3(3): e201900547.

Stoffel EM and Murphy CC (2020) Epidemiology and mechanisms of the increasing incidence of colon and rectal cancers in young adults. Gastroenterology. 158(2):341-353.

Yoshizawa-Sugata N and Masai H (2009) Roles of human AND-1 in chromosome transactions in S phase. The Journal of Biological Chemistry284(31):20718-20728.

Yu Z, Bai X, Zhou R, et al. (2024) Differences in the incidence and mortality of digestive cancer between Global Cancer Observatory 2020 and Global Burden of Disease 2019. International Journal of Cancer154(4):615-625.

Yuan JP, Zeng W, Huang GN, e al. (2007) STIM1 heteromultimerizes TRPC channels to determine their function as store-operated channels. Nature Cell Biology9(6):636–645.

Zhou Y and Chen JJ (2021) STAT3 plays an important role in DNA replication by turning on WDHD1. Cell &Bioscience11(1):10.

Zhu W, Ukomadu C, Jha S, Set al. (2007) Mcm10 and And-1/CTF4 recruit DNA polymerase alpha to chromatin for initiation of DNA replication. Genes &Development;21(18):2288-2299.

Supplementary Files

This is a list of supplementary files associated with this preprint. Click to download.

- Table1.docx
- Table2.docx
- Westernblotrawdata.zip